

# Generation of spin current by Coulomb drag

M. Pustilnik,<sup>1</sup> E.G. Mishchenko,<sup>2</sup> and O.A. Starykh<sup>2</sup>

<sup>1</sup>*School of Physics, Georgia Institute of Technology, Atlanta, GA 30332*

<sup>2</sup>*Department of Physics, University of Utah, Salt Lake City, UT 84112*

Coulomb drag between two quantum wires is exponentially sensitive to the mismatch of their electronic densities. The application of a magnetic field can compensate this mismatch for electrons of opposite spin directions in different wires. The resulting enhanced momentum transfer leads to the conversion of the charge current in the active wire to the spin current in the passive wire.

PACS numbers: 71.10.Pm, 73.63.Nm

A set of unusual transport phenomena in which electron-electron interactions induce transfer of momentum between distinguishable systems of fermions is known as Coulomb drag effect. Conventional Coulomb drag [1] occurs between two spatially separated conductors. In the standard setup, see Fig. 1, dc current  $I_1$  flows through the *active* conductor 1 inducing a voltage drop  $V_2$  in the *passive* conductor 2. Quantitatively, the effect is characterized by the dimensionless *drag resistance*

$$R_d = \lim_{I_1 \rightarrow 0} (e^2/h)V_2/I_1. \quad (1)$$

Unlike the usual two-terminal resistance,  $R_d$  is sensitive to electronic correlations within the conductors. Therefore, Coulomb drag effect provides an important tool to probe these correlations. Coulomb drag was observed experimentally in two-dimensional bilayers [2] and, more recently, in one-dimensional quantum wires [3].

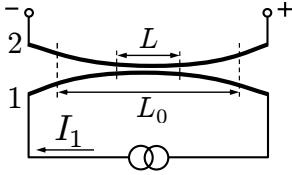


FIG. 1: Equivalent circuit for measurement of Coulomb drag between two quantum wires. Coulomb drag manifests itself in the appearance of the potential difference  $V_2$  between the ends of the open circuit of which the passive wire 2 is a part ( $V_2$  is positive if it has the polarity indicated).

A different Coulomb drag-type effect, the *spin drag*, originates in momentum transfer between spin-up and spin-down electrons *within the same conductor* [4]. The spin drag provides a non-dissipative mechanism of relaxation of a pure spin current. Interactions are therefore *destructive* for spin currents. Because robust generation of spin currents is important in view of possible applications in spintronics [5], the limitations arising due to the spin drag effect are now a subject of active research [4, 6].

In this paper we demonstrate that interactions can *induce* spin current rather than suppress it. This is possible in a novel type of Coulomb drag effect, interaction-induced transfer of momentum between spin-up and spin-down electrons that belong to *separate* conductors. We

show that this effect can be realized in the standard setting of Coulomb drag between two clean quantum wires in a magnetic field [3]. While the electric current  $I_2$  in the passive wire is zero, the spin current  $I_{2s} = I_{2\uparrow} - I_{2\downarrow}$  can flow [7], i.e. the system acts as a *charge current to spin current converter*. The efficiency of the conversion can be characterized by the ratio

$$C = I_{2s}/I_1. \quad (2)$$

Below we show that the drag resistance  $R_d$  has a maximum at a certain value  $B_0$  of Zeeman energy. For

$$\max\{T, |B - B_0|\} \ll B_0 \quad (3)$$

the conversion efficiency  $C \sim R_d$  [see Eqs. (18) and (23)], and the dependence of  $R_d$  on temperature  $T$  is described by a power law with the exponent depending on the interaction strength, see Eq. (15). For sufficiently strong interaction the power-law dependence crosses over to  $R_d \sim 1$  at very low temperatures. We start with a heuristic explanation of the origin of the effect, and then proceed with the derivation of the results.

If the electronic densities in the wires  $n_1$  and  $n_2$  were equal, the dominant contribution to  $R_d$  at low temperatures would come from processes with large momentum transfer between the wires (backscattering), which may result in a finite  $R_d$  in the limit  $T \rightarrow 0$  [8, 9, 10]. In reality, however, the densities are always slightly different,

$$|n_1 - n_2| \ll n, \quad n = (n_1 + n_2)/2$$

(let us assume that  $n_1 < n_2$ ), so that the corresponding Fermi momenta  $k_{1,2} = \pi n_{1,2}/2$  are different as well. In this case, the backscattering contribution to  $R_d$  is exponentially suppressed at low temperatures [11, 12].

The suppression is easy to understand as follows. To the lowest order in the strength of the interwire interaction, the backscattering contribution to  $R_d$  can be written as [12, 13]

$$\frac{R_d}{L} \sim \frac{U_{2k}^2}{T} \int dq \int_0^\infty d\omega e^{-\omega/T} \prod_i S_i^{2k}(q, \omega) \quad (4)$$

Here  $L$  is the length of the region in which the wires interact with each other (see Fig. 1),  $U_{2k}$  is  $2k$ -Fourier

component of the interwire interaction potential (with  $k = (k_1 + k_2)/2 = \pi n/2$ ), and  $S_i^{2k}(q, \omega) = S_i(q, \omega)|_{q \sim 2k}$  is the Fourier transform of the dynamic structure factor  $S_i(x, t) = \langle \rho_i(x, t) \rho_i(0, 0) \rangle$  (here  $\rho_i$  is the local density operator for wire  $i$ ).

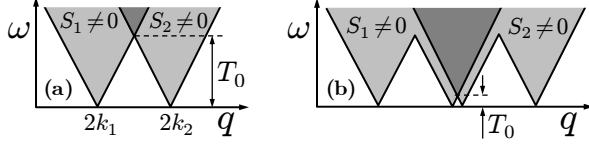


FIG. 2: (a) Regions in  $(\omega, q)$ -plane where  $S_{1,2} > 0$  at  $T = 0$  and  $q \sim 2k$ . The dark triangle indicates the region where  $S_1 S_2 > 0$ . (b) In a magnetic field, the low-energy sectors in  $S_i(q, \omega)$  split in two, which leads to the decrease of  $T_0$ , the minimal energy at which  $S_1$  and  $S_2$  overlap at  $T = 0$ .

At  $T = 0$  and  $q \sim 2k$ , the two structure factors overlap only at  $\omega > T_0 \sim v|k_1 - k_2|$ , where  $v = \pi n/2m$  is the “average” Fermi velocity, see Fig. 2(a). Because of the factor  $e^{-\omega/T}$  in Eq. (4), this translates to the activational temperature dependence of the drag resistance,  $R_d \propto e^{-T_0/T}$ . Although at any  $T > 0$  the structure factors are finite for all  $\omega$  and  $q$ , the “leakage” of the spectral weight beyond the boundaries indicated in Fig. 2(a) affects only the power-law prefactor in the expression for  $R_d$ .

With the backscattering contribution exponentially suppressed,  $R_d$  is dominated by small momentum transfer and vanishes at  $T \rightarrow 0$  as  $R_d \propto T^5$  [12]. In principle, the densities can be fine-tuned to be equal, which would increase the backscattering contribution. Another possibility, which leads to spin current generation, is to place the system in a magnetic field.

In a field the single-particle energies  $\xi_{k\sigma}$  of the spin-up ( $\uparrow$ ) and spin-down ( $\downarrow$ ) electrons (labeled by  $\sigma = \pm 1$ ) include Zeeman contribution  $\delta\xi_{k\sigma} = \sigma B/2$ . As a result,  $n_{i\downarrow} > n_{i\uparrow}$ , and the Fermi momenta are

$$k_{i\sigma} = k_i - \sigma \delta k/2 \quad (5)$$

with  $\delta k(B) \sim B/v$  (see below). For each wire, the low-energy sector in  $S_i^{2k}(q, \omega)$  then splits in two, located at  $q = 2k_{i\sigma}$ , see Fig. 2(b). The scale  $T_0$  is  $B$ -dependent and vanishes at a certain field  $B_0$ ,  $T_0(B) \sim |B - B_0|$  (see Eq. (11) below). At  $|B - B_0| \lesssim T$ , the backscattering contribution to  $R_d$  is no longer exponentially suppressed and dominates at sufficiently low temperatures. Moreover, in the regime (3) the main contribution to the integral in Eq. (4) comes from the overlap of  $S_{1\downarrow}$  and  $S_{2\uparrow}$ . In other words, *almost all of the momentum is transferred from spin-down electrons in the active wire to spin-up electrons in the passive one*. Therefore, both  $R_d$  and  $C$  will have a maximum at  $B = B_0$ .

We evaluate  $R_d$  and  $C$  in the regime (3) using the bosonization technique [14]. At energies well below  $B_0$ , which in turn is small compared with the Fermi energy

$\epsilon_F$ , the wire  $i$  ( $i = 1, 2$ ) is described by the Hamiltonian

$$H_i = \sum_m \frac{v_m}{2} \int dx [g_m^{-1} (\partial_x \varphi_{im})^2 + g_m (\partial_x \vartheta_{im})^2], \quad (6)$$

where  $m = c, s$  labels the charge (spin) modes, and the bosonic fields satisfy

$$[\varphi_{im}(x), \vartheta_{i'm'}(y)] = (i/2) \delta_{ii'} \delta_{mm'} \text{sgn}(x - y). \quad (7)$$

For simplicity, we assume that both wires are described by the same set of parameters  $\{v_m, g_m\}$ . These parameters are related to each other according to

$$g_c = v/v_c, \quad g_s(B_0) = 1 + [2 \ln(\epsilon_F/B_0)]^{-1} \quad (8)$$

(so that  $1 - g_c \gg g_s - 1 > 0$  for  $B_0 \ll \epsilon_F$ ), and the velocities  $v_c > v$  and  $v_s < v$  can be further expressed in terms of the interaction within the wires [14].

Fermion operators in the bosonic representation are

$$\psi_{i\alpha\sigma}(x) = \mu_{i\alpha\sigma} \sqrt{p_0} e^{i\alpha[\eta_{i\alpha\sigma}(x) + k_{i\sigma}x]}. \quad (9)$$

Here  $\alpha = +1(-1)$  for the right (left) moving fermions,  $\mu_{i\alpha\sigma} = \mu_{i\alpha\sigma}^\dagger$  are real (Majorana) fermions that satisfy  $\{\mu_{i\alpha\sigma}, \mu_{i'\alpha'\sigma'}\} = 2\delta_{ii'} \delta_{\alpha\alpha'} \delta_{\sigma\sigma'}$  (these operators enforce correct anticommutation relations between different fermionic species),  $p_0 \sim B_0/v$  is the high-momentum cutoff, and  $\eta_{i\alpha\sigma}$  is a linear combination of  $\varphi_{im}, \vartheta_{im}$ , which in the leading order in  $B_0/\epsilon_F \ll 1$  is given by [15]

$$\eta_{i\alpha\sigma} = \sqrt{\pi/2} (\varphi_{ic} + \alpha \vartheta_{ic} + \sigma \varphi_{is} + \alpha \sigma \vartheta_{is}). \quad (10)$$

Fermi momenta  $k_{i\sigma}$  in Eq. (9) are given by Eq. (5) with  $\delta k(B) = g_s B/v_s$ , and  $T_0(B)$  (see Fig. 2) at  $B \rightarrow B_0$  is

$$T_0(B) \approx g_s |B - B_0|, \quad B_0 \approx v_s |k_2 - k_1| \quad (11)$$

( $B_0$  is the root of the equation  $g_s(B)B = v_s |k_2 - k_1|$ ).

With the help of Eq. (9), the  $2k$ -harmonic of the density operator  $\rho_i^{2k} = \sum_\sigma \rho_{i\sigma}^{2k}$  is written as

$$\rho_{i\sigma}^{2k} = p_0 \mu_{i\sigma} \exp[i\sqrt{2\pi} (\varphi_{ic} + \sigma \varphi_{is}) + 2ik_{i\sigma}x] + \text{H.c.},$$

where  $\mu_{i\sigma} = \mu_{i,-1,\sigma} \mu_{i,+1,\sigma}$ . Since the Hamiltonian (6) is quadratic, evaluation of the structure factor is straightforward [14] and yields  $S_i(x, t) = \sum_\sigma S_{i\sigma}(x, t)$  with

$$S_{i\sigma}(x, t) = 2p_0^2 \cos(2k_{i\sigma}x) \prod_{\alpha,m} \left[ \frac{T/(2p_0 v_m)}{\sinh(\pi T \tau_{\alpha m})} \right]^{g_m/2},$$

where  $\tau_{\alpha m} = x/v_m - \alpha(t - i0)$ .

As discussed above, the condition (3) ensures that the main contribution to the integral in Eq. (4) comes from the nonvanishing overlap of  $S_{1\downarrow}$  and  $S_{2\uparrow}$ ; the remaining contributions are suppressed as  $\propto \exp(-B_0/T)$ . In order to evaluate  $R_d$ , it is convenient to convert Eq. (4) to space-time representation,

$$R_d/L = (\pi/2) U_{2k}^2 \int_{-\infty}^{\infty} dx dt (it) S_1(x, t) S_2(x, t). \quad (12)$$

Substituting here  $S_{1\downarrow}$  for  $S_1$  and  $S_{2\uparrow}$  for  $S_2$ , we find

$$R_d \sim n\lambda_{2k}^2 L \frac{B_0}{\epsilon_F} \left[ \frac{|B - B_0|}{B_0} \right]^{4g-3} F\left(\frac{g_s|B - B_0|}{T}\right), \quad (13)$$

where  $\lambda_{2k} = U_{2k}/2\pi v$  and  $g = (g_c + g_s)/2$ . The function  $F(z)$  in Eq. (13) is given by

$$F(z) = \iint \frac{(z/2)^{3-4g} \exp(2iz\xi/\pi) d\xi d\zeta}{\prod_m [\cosh(\frac{v_s}{v_m} \xi + \zeta) \cosh(\frac{v_s}{v_m} \xi - \zeta)]^{g_m}} \sim \begin{cases} z^{3-4g}, & z \ll 1 \\ ze^{-z}, & 1 \ll z \ll z_0 \\ z^{1-2g_c} e^{-z}, & z \gg z_0 \end{cases}, \quad (14)$$

where  $z_0 = g_c(\pi/2)(v_s/v_c) \tan[(\pi/2)(v_s/v_c)]$  (so that  $z_0 \sim (1 - g_c)^{-1} \gg 1$  for weak interaction). In deriving Eqs. (13),(14) we changed the integration variables in (12) to  $\xi = \pi T x/v_s$  and  $\zeta = \pi T t$ , shifted the path of integration over  $\zeta$  off the real axis by  $-i\pi/2$ , and evaluated the resulting integral in the saddle-point approximation. According to Eqs. (13),(14), and in agreement with the discussion above,  $R_d(B)$  has a narrow peak of the width  $\delta B \sim T \ll B_0$  at  $B = B_0$ . Its height is given by

$$\max\{R_d(B)\} \sim n\lambda_{2k}^2 L (B_0/\epsilon_F)(T/B_0)^{4g-3}. \quad (15)$$

Note that the difference between  $v_s$  and  $v_c$  is important only at large  $|B - B_0| \gtrsim T/(1 - g_c)$ . In the opposite limit one can set  $v_s/v_c \rightarrow 1$ , which yields  $F(z) = |\Gamma(g + iz/2\pi)|^4/\Gamma^2(2g)$ , in agreement with Eq. (14); the corresponding  $T$ -dependence is exactly the same as that for the drag between two spinless wires [11, 16].

In order to relate the conversion efficiency (2) to the drag resistance (15), we note that as far as the passive wire is concerned, in the regime (3) Coulomb drag induces the electric field that couples to spin-up electrons only. The effect of this field can be described by adding to the Hamiltonian of the passive wire a term

$$\delta H_2 = e \int dx \Phi_d(x) \rho_{2\uparrow}(x) = e \int dx \frac{\Phi_d}{2} (\rho_{2c} + \rho_{2s}), \quad (16)$$

where  $\Phi_d(x)$  is drag-induced potential, and  $\rho_{2c}$  and  $\rho_{2s}$  are charge and spin densities. The potential  $\Phi_d(x)$  changes within the region of the length  $L$  in which the wires interact with each other. Assuming that the wires are long,  $L_0 \gg L$ , the charge and spin currents in response to  $\delta H_2$  can be written as [17]

$$I_{2c} = (2e^2/h) g_c \delta\Phi_d/2, \quad I_{2s} = (2e^2/h) g_s \delta\Phi_d/2, \quad (17)$$

where  $\delta\Phi_d = \Phi_d(-\infty) - \Phi_d(\infty)$ . In writing Eq. (17) we took into account the renormalization of the corresponding conductances by interactions within the wire [17].

On the other hand, the electrostatic potential difference  $V_2$  induces charge current  $I_V = (2e^2/h)V_2$ . Here we assumed that the interactions are efficiently screened

within the leads and that the contacts between the leads and the wires are reflectionless; the corresponding conductance is not affected by the interactions [18]. The condition of vanishing of the total electric current,  $I_2 = I_V + I_{2c} = 0$ , then yields  $\delta\Phi_d = -2V_2/g_c$ . Eqs. (1),(2) and (17) now give

$$C = I_{2s}/I_1 = 2(g_s/g_c)R_d. \quad (18)$$

Thus, under the conditions (3) the dependence of conversion efficiency  $C$  on  $B$  and  $T$  is indeed the same as that of the drag resistance  $R_d$ , as asserted above.

Eq. (18) does not account for the reduction of  $I_s$  due to the momentum transfer between the two spin subsystems within the passive wire (spin drag). Indeed, in the framework of the Tomonaga-Luttinger model (6) the only source of spin drag is the backscattering in the spin sector, which at  $T \ll B$  is exponentially suppressed. The dominant contribution to spin drag then comes from the processes with small momentum transfer. Accounting for these processes requires explicit consideration of the nonlinearity of the electronic spectrum [12]. Proceeding along the lines of [12], we found the corresponding correction to the spin current  $I_{2s}$  at  $T \ll B$  and in the lowest non-vanishing order in the interaction strength,

$$\delta I_{2s}/I_{2s} \sim -nL_0(1 - g_c)^4(B/\epsilon_F)^4(T/B)^5. \quad (19)$$

In writing Eq. (19) we took into account that Fermi velocities for spin-up and spin-down electrons differ by  $\delta v \sim B/k \ll v$ . The correction (19) is small and does not affect the validity of Eq. (18).

The above consideration is based on the perturbative expression Eq. (4). In order to analyze the relevance of the higher-order contributions, we introduce new fields

$$\phi_c = 2^{-1/2}(\varphi_{1c} - \varphi_{2c}), \quad \phi_s = 2^{-1/2}(\varphi_{1s} + \varphi_{2s}),$$

and similarly defined  $\theta_c$  and  $\theta_s$ . The fields obey the commutation relations analogous to Eq. (7), and their dynamics is governed by the Hamiltonian  $H = \int dx \mathcal{H}$  with

$$\mathcal{H} = \sum_m \frac{v_m}{2} [g_m^{-1}(\partial_x \phi_m)^2 + g_m(\partial_x \theta_m)^2] - 2v\lambda_0(\partial_x \phi_c)^2 + 4\pi v\lambda_{2k}p_0^2 \cos\left\{\sqrt{4\pi}(\phi_c - \phi_s) + 2K_0x\right\}. \quad (20)$$

The second and the third terms here describe, respectively, the forward and backward scattering between the spin-up electrons in wire 2 and the spin-down electrons in wire 1, with  $\lambda_0$  defined similarly to  $\lambda_{2k}$  in Eq. (13), and  $K_0 = T_0(B)/v_s$ .

The forward scattering term in Eq. (20) leads to small corrections to  $v_c$  and  $g_c$ ,  $\delta g_c/g_c \approx -\delta v_c/v_c \approx 2g_c^2\lambda_0 \ll 1$ , which modify the exponent in Eqs. (13)-(15),  $g \rightarrow g + \delta g_c/2$ . The backscattering, however, can be relevant in the renormalization group sense [19]. For  $L \rightarrow \infty$  and  $K_0 \rightarrow 0$  it then results in the opening of a gap

$$\Delta \sim B_0\lambda_{2k}^{1/(2-2g)} \quad (21)$$

in the excitation spectrum. The gapped state is the “zigzag”-ordered state formed by the spin-down electrons in wire 1 and the spin-up electrons in wire 2.

The gap remains open for finite  $K_0$  as long as the energy gained due to its formation is sufficient to overcome the cost of the adjustment of the densities needed to form the zigzag order. In the context of quantum wires such adjustment (known as commensurate-incommensurate transition) was discussed recently in [11, 20]. The adjustment takes place at not too large  $K_0$ ,  $K_0 < K_c \sim \Delta/v$ , and occurs even when  $L$  is finite. As a result, the width  $\delta B$  of the peak in  $R_d(B)$  saturates at low temperatures,

$$\delta B \sim \max\{T, \Delta\}. \quad (22)$$

For  $L \ll v/\Delta$  the zigzag order can not be formed and Eq. (15) is applicable. In this case  $\max\{R_d(B)\} \ll 1$  for all  $T$ . The higher-order contributions become important for  $L \gtrsim v/\Delta$  and at  $T \lesssim \Delta$  [8, 9, 10, 11]. While finding the detailed dependence  $R_d(T)$  in this regime is beyond the scope of this Letter, the limiting values of  $R_d$  and  $C$  at  $T \rightarrow 0$  can be found as follows. Imagine that the two wires are connected to noninteracting reservoirs and a bias is applied only to the electrons with spin  $\sigma$  in wire  $i$ . The resulting current of electrons with spin  $\sigma'$  in wire  $i'$  is  $I_{i'\sigma'} = G_{i'\sigma',i\sigma} V_{i\sigma}$ , where  $G_{i'\sigma',i\sigma} = G_{i\sigma,i'\sigma'}$  is the corresponding conductance. At  $T \rightarrow 0$  the spin-up electrons in wire 2 are “locked” with the spin-down electrons in wire 1, and we expect that  $G_{1\downarrow,1\downarrow}, G_{2\uparrow,2\uparrow}, G_{1\downarrow,2\uparrow} \rightarrow e^2/2h$ . At the same time,  $G_{1\uparrow,1\uparrow}, G_{2\downarrow,2\downarrow} \rightarrow e^2/h$ , while  $G_{1\uparrow,2\downarrow} \rightarrow 0$ . Setting  $V_{i\sigma} = V_i$ ,  $I_i = I_{i\uparrow} + I_{i\downarrow}$ , we find

$$R_d \rightarrow 1/4, \quad C \rightarrow 1/2. \quad (23)$$

To conclude, we showed that in the presence of the applied magnetic field the standard Coulomb drag measurement setup acts as a charge current to spin current converter. Both the drag resistance and the conversion efficiency exhibit a maximum at a certain value of the field controlled by the density mismatch between the wires.

Our results are applicable for long ( $kL_0 \gg 1$ ) ballistic quantum wires. The wires studied in [3] exhibit a well-defined conductance quantization, which guarantees that the elastic mean free path exceeds the length of the wires  $L_0$ . While it is very plausible that  $kL_0 \gg 1$  for at least some of the samples studied in [3] (with  $L_0$  ranging from  $0.4 \mu\text{m}$  to  $4 \mu\text{m}$ ), the density of electrons in these wires is difficult to estimate. Fortunately, such estimate is available for the coupled-wire system studied in [21]:  $L \approx L_0 \approx 10 \mu\text{m}$  and  $kL_0 \sim 10^3$ . Although the experiments [21] focus on the momentum-resolved tunneling, the same system can be employed to study the Coulomb drag effect as well. For this system, the typical density mismatch  $|n_1 - n_2|/n \sim 10^{-2}$  corresponds to  $B_0 \sim 1$  K (which amounts to the applied field of  $\sim 3$  Tesla), hence the regime (3) is well within the reach of the experiments.

We thank L. Glazman and G. Vignale for useful discussions. MP and EGM are grateful to the Kavli Institute for Theoretical Physics at UCSB and MP thanks the Aspen Center for Physics for their hospitality. This work is supported by the NSF (grants DMR-0503172 and DMR-0604107), by the DOE (grants DE-FG02-ER46311 and DE-FG02-06ER46313), and by the ACS PRF (grant 43219-AC10).

- 
- [1] M.B. Pogrebinskii, Sov. Phys. Semicond. **11**, 372 (1977); P.J. Price, Physica B **117**, 750 (1983).
  - [2] P.M. Solomon *et al.*, Phys. Rev. Lett. **63**, 2508 (1989); T.J. Gramila *et al.*, Phys. Rev. Lett. **66**, 1216 (1991); U. Sivan *et al.*, Phys. Rev. Lett. **68**, 1196 (1992).
  - [3] P. Debray *et al.*, J. Phys. Condens. Matter **13**, 3389 (2001); M. Yamamoto *et al.*, Physica E **12**, 726 (2002); M. Yamamoto *et al.*, Science **313**, 204 (2006).
  - [4] I. D’Amico and G. Vignale, Phys. Rev. B **62**, 4853 (2000); Europhys. Lett. **55**, 566 (2001); K. Flensberg, T.S. Jensen, and N.A. Mortensen, Phys. Rev. B **64**, 245308 (2001).
  - [5] I. Žutić, J. Fabian, and S. Das Sarma, Rev. Mod. Phys. **76**, 323 (2004).
  - [6] C.P. Weber *et al.*, Nature **437**, 1330 (2005).
  - [7] A spin current  $I_s$  in a wire leads to the spin accumulation  $M = N_\uparrow - N_\downarrow \neq 0$  in the reservoirs to which the wire is attached ( $N_\sigma$  is number of electrons with spin  $\sigma$  in the reservoir). In the steady state  $M = I_s \tau / e$ , where  $1/\tau$  is the spin relaxation rate in the reservoirs.
  - [8] Yu.V. Nazarov and D.V. Averin, Phys. Rev. Lett. **81**, 653 (1998).
  - [9] K. Flensberg, Phys. Rev. Lett. **81**, 184 (1998).
  - [10] R. Klesse and A. Stern, Phys. Rev. B **62**, 16912 (2000).
  - [11] T. Fuchs, R. Klesse, and A. Stern, Phys. Rev. B **71**, 045321 (2005).
  - [12] M. Pustilnik *et al.*, Phys. Rev. Lett. **91**, 126805 (2003).
  - [13] L. Zheng and A.H. MacDonald, Phys. Rev. B **48**, 8203 (1993).
  - [14] T. Giamarchi, *Quantum Physics in One Dimension* (Oxford University Press, 2004).
  - [15] T. Hikihara, A. Furusaki, and K.A. Matveev, Phys. Rev. B **72**, 035301 (2005); K. Penc and J. Sólyom, Phys. Rev. B **47**, 6273 (1993).
  - [16] G.A. Fiete, K. Le Hur, and L. Balents, Phys. Rev. B **73**, 165104 (2006).
  - [17] C.L. Kane and M.P.A. Fisher, Phys. Rev. Lett. **68**, 1220 (1992); Phys. Rev. B **46**, 15233 (1992).
  - [18] D.L. Maslov and M. Stone, Phys. Rev. B **52**, R5539 (1995); V.V. Ponomarenko, Phys. Rev. B **52**, R8666 (1995); I. Safi and H. J. Schulz, Phys. Rev. B **52**, R17040 (1995).
  - [19] By power counting, the backscattering in Eq. (20) is relevant if  $g < 1$ . For weak interaction and large interwire separation  $\lambda_0 \ll 1 - g_c \ll 1$ , and  $g < 1$  at any  $B \ll \epsilon_F$ . For small interwire separation the situation is more delicate and requires the analysis of the RG flow similar to that in Ref. [10] at  $B = 0$ .
  - [20] O.A. Starykh *et al.*, Lecture Notes Phys. **544**, 37 (2000).
  - [21] O.M. Auslender *et al.*, Science **295**, 825 (2002); O.M. Auslender *et al.*, Sol. State Commun. **131**, 657 (2004).